

# Peroxisome proliferator-activated receptor $\alpha$ activation attenuates the inflammatory response to protect the liver from acute failure by promoting the autophagy pathway

M Jiao<sup>1,2,6</sup>, F Ren<sup>3,2,6</sup>, L Zhou<sup>2</sup>, X Zhang<sup>3</sup>, L Zhang<sup>1</sup>, T Wen<sup>3</sup>, L Wei<sup>2</sup>, X Wang<sup>4</sup>, H Shi<sup>3</sup>, L Bai<sup>2</sup>, X Zhang<sup>2</sup>, S Zheng<sup>2</sup>, J Zhang<sup>2</sup>, Y Chen<sup>2</sup>, Y Han<sup>5</sup>, C Zhao<sup>\*1</sup> and Z Duan<sup>\*2</sup>

Peroxisome proliferator-activated receptor  $\alpha$  (PPAR $\alpha$ ) has been reported to induce a potent anti-inflammatory response. Autophagy is a recently recognized rudimentary cellular response to inflammation and injury. The aim of the present study was to test the hypothesis that PPAR $\alpha$  activation mediates autophagy to inhibit liver inflammation and protect against acute liver failure (ALF). PPAR $\alpha$  expression during ALF and the impact of PPAR $\alpha$  activation by Wy-14 643 on the hepatic immune response were studied in a D-galactosamine/lipopolysaccharide-induced mouse model. Autophagy was inhibited by 3-methyladenine or small interfering RNA (siRNA) against Atg7. In both the mouse model and human ALF subjects, PPAR $\alpha$  was significantly downregulated in the injured liver. PPAR $\alpha$  activation by pretreatment with Wy-14 643 protected against liver injury in mice. The protective effect of PPAR $\alpha$  activation relied on the suppression of inflammatory mechanisms through the induction of autophagy. This hypothesis is supported by the following evidence: first, PPAR $\alpha$  activation suppressed proinflammatory responses and inhibited phosphorylated NF- $\kappa$ Bp65, phosphorylated JNK and phosphorylated ERK pathways *in vivo*. Second, protection by PPAR $\alpha$  activation was due to the induction of autophagy because inhibition of autophagy by 3-methyladenine or Atg7 siRNA reversed liver protection and inflammation. Third, PPAR $\alpha$  activation directly induced autophagy in primary macrophages *in vitro*, which protected cells from a lipopolysaccharide-induced proinflammatory response. Here, for the first time, we have demonstrated that PPAR $\alpha$ -mediated induction of autophagy ameliorated liver injury in cases of ALF by attenuating inflammatory responses, indicating a potential therapeutic application for ALF treatment.

*Cell Death and Disease* (2014) 5, e1397; doi:10.1038/cddis.2014.361; published online 28 August 2014

Acute liver failure (ALF), an inflammation-mediated hepatocellular injury process, is a clinical syndrome that results from hepatocellular apoptosis and hemorrhagic necrosis.<sup>1</sup> ALF frequently results from viral hepatitis, ingestion of drugs or toxic substances, or hepatic ischemia–reperfusion injury, among others. The prognosis for ALF is extremely poor, and there is currently no effective therapy for the end stage of the disease other than liver transplantation.<sup>2</sup> Although the nature of ALF has been extensively studied, the mechanisms by which organ damage occurs are not completely understood.

Peroxisome proliferator-activated receptors (PPARs) are members of the nuclear hormone receptor superfamily of ligand-activated transcription factors, with its subfamily consisting of three members: PPAR $\alpha$ , PPAR $\beta$  and PPAR $\gamma$ .<sup>3,4</sup>

PPAR $\alpha$  has been reported to be involved in a number of cellular processes, including lipid and lipoprotein metabolism,<sup>5</sup> apoptosis<sup>6</sup> and inflammatory responses.<sup>7–9</sup> Studies have demonstrated that PPAR $\alpha$  exhibits potent anti-inflammatory activity through suppressing nuclear factor- $\kappa$ B (NF- $\kappa$ B) and/or modulating the activation (phosphorylation) of signal transducer and activator of transcription1 (STAT1)-related inflammatory signaling in cultured neuronal cells.<sup>7,10</sup> PPAR $\alpha$ -null mice exhibit an aggravated reaction to various inflammatory stimuli in the skin, blood vessels, intestine and lung.<sup>11–14</sup> Recently, in a model of lipopolysaccharide (LPS)-induced hepatic inflammatory injury, reduced PPAR $\alpha$  expression was shown to be associated with increased tissue bacterial load in sepsis.<sup>15</sup> Additionally, a lack of PPAR $\alpha$

<sup>1</sup>Department of Infectious Diseases, The Third Affiliated Hospital of Hebei Medical University, Shijiazhuang, China; <sup>2</sup>Beijing Artificial Liver Treatment and Training Center, Beijing YouAn Hospital, Capital Medical University, Beijing, China; <sup>3</sup>Beijing Institute of Hepatology, Beijing YouAn Hospital, Capital Medical University, Beijing, China; <sup>4</sup>Department of Pathology, Beijing YouAn Hospital, Capital Medical University, Beijing, China and <sup>5</sup>Sichuan University, The College of Life Sciences, Chengdu, China

\*Corresponding authors: C Zhao, Department of Infectious Diseases, The Third Affiliated Hospital of Hebei Medical University, Shijiazhuang 050051, China. Tel: +86 10 83997726; Fax: +86 10 63295285; E-mail: zhaocy2005@163.com or Z Duan, Beijing Artificial Liver Treatment and Training Center, Beijing YouAn Hospital, Capital Medical University, Beijing 100069, China. Tel: +86 10 63291007; Fax: +86 10 63295285; E-mail: duanzhongping0929@hotmail.com

<sup>6</sup>These authors contributed equally to this work.

**Abbreviations:** ALF, acute liver failure; PPAR $\alpha$ , peroxisome proliferator-activated receptor  $\alpha$ ; D-GalN, D-galactosamine; LPS, lipopolysaccharide; NF- $\kappa$ B, nuclear factor- $\kappa$ B; MAPK, mitogen-activated protein kinase; STAT1, signal transducer and activator of transcription 1; TNF- $\alpha$ , tumor necrosis factor- $\alpha$ ; ALT, alanine aminotransferase; AST, aspartate aminotransferase; MPO, myeloperoxidase; CHB, chronic hepatitis B; TLR4, toll-like receptor 4; BMDM, bone marrow-derived macrophage; 3-MA, 3-methyladenine; Atg, autophagy gene; CCL, chemokine (C–C motif) ligand; CXCL, chemokine (C–X–C motif) ligand; IL-1 $\beta$ , interleukin-1 $\beta$ ; iNOS, inducible nitric oxide synthase; CQ, chloroquine; qRT-PCR, quantitative reverse transcription PCR; HBV, hepatitis B virus

Received 21.12.13; revised 19.7.14; accepted 21.7.14; Edited by GM Fimia

exacerbates LPS-induced liver toxicity through STAT1 inflammatory signaling and increases oxidative/nitrosative stress.<sup>16</sup> However, the functional role of PPAR $\alpha$  in the pathogenesis of ALF remains elusive. An ALF model induced by the coinjection of D-galactosamine (D-GalN) and LPS has been widely used to examine the underlying mechanisms of ALF.<sup>17,18</sup> In the present study, we used D-GalN/LPS to induce ALF in mice and to explore the roles of PPAR $\alpha$  in the context of ALF.

Macroautophagy (referred to hereafter as autophagy) is a highly evolutionarily conserved process found in virtually all types of eukaryotic cells. Autophagy involves the sequestration of regions of cytosol within double-membrane-bound compartments followed by lysosome-based degradation of the contents. Previous studies have suggested that autophagy represents an adaptive strategy by which cells can remove damaged organelles and enhance survival following bioenergetics-induced stress.<sup>19–21</sup> In addition, accumulating evidence has demonstrated multiple roles of autophagy in the regulation of cell death, differentiation and the anti-microbial response in mammals.<sup>20,21</sup> In recent years, emerging evidence has indicated that the autophagy process may have an essential role for the host during bacterial clearance and may also interact with inflammatory processes, which consequently may impact the outcomes of disease progression.<sup>22,23</sup> There is a complex reciprocal relationship between autophagy pathway/proteins and inflammation.<sup>24,25</sup> Recent observations have revealed a relationship between autophagy and inflammasome-associated proinflammatory cytokine maturation in macrophages.<sup>26,27</sup>

Given the above information, we speculated that PPAR $\alpha$  activation may serve as a protective function to restrain liver inflammation in cases of ALF. Moreover, we further hypothesized that PPAR $\alpha$  activation attenuates inflammatory response by regulating autophagy in ALF. In the present study, PPAR $\alpha$  activation protected mice from D-GalN/LPS-induced ALF and significantly downregulated the expression of proinflammatory cytokines. Moreover, PPAR $\alpha$  activation resulted in elevated autophagy induced by D-GalN/LPS in mice, and autophagy inhibition by 3-methyladenine (3-MA) or Atg7 siRNA reversed the hepatoprotective effect of PPAR $\alpha$  activation and restored the inflammatory response in ALF mice. Hence, by orchestrating autophagy signaling, PPAR $\alpha$  is essential for the inflammation mechanism in the ALF immune response cascade.

## Results

**Intrahepatic expression of PPAR $\alpha$  is suppressed in D-GalN/LPS-induced ALF.** According to the pathologic characteristics of liver and the levels of serum transaminase, massive hepatic injury was apparent after 4–6 h as determined by hematoxylin and eosin (H&E) staining (Figure 1a), which was in agreement with the increased serum alanine aminotransferase (ALT) and aspartate aminotransferase (AST) enzyme levels (Figure 1b); thus, the mice ALF model is successfully formatted at 6 h after D-GalN/LPS injection. Next, we investigated a possible association between PPAR $\alpha$  and ALF induced by D-GalN/LPS treatment. Accompanying the liver injury, PPAR $\alpha$  mRNA and protein levels

gradually declined over the same time period (Figure 1c and Supplementary Figure 1). These results indicated that PPAR $\alpha$  is suppressed with the gradual progression of D-GalN/LPS-induced ALF.

**PPAR $\alpha$  activation protects against D-GalN/LPS-induced ALF, which is associated with suppressed hepatic inflammation.** We then evaluated whether PPAR $\alpha$  activation could rescue the injury by applying Wy-14 643, a PPAR $\alpha$  ligand activator. Pretreatment with Wy-14 643 for 2 h before D-GalN/LPS treatment resulted in complete protection against ALF. In the survival analysis, the mice in the D-GalN/LPS control group began to perish 6 h after D-GalN/LPS injection, and the survival rate of these mice was 30% (3 of 10 mice) at the 48-h time point. By contrast, the survival rate after Wy-14 643 treatment was 70% (7 of 10 mice; Figure 2a). The gross morphology of the liver after Wy-14 643 treatment appeared substantially normal, and the liver architecture was well preserved (Figure 2b). With respect to liver damage, the mice subjected to Wy-14 643 treatment showed significantly lower sALT and sAST levels compared with the ALF group (Figure 2c). These results demonstrated that PPAR $\alpha$  is critical for D-GalN/LPS-induced ALF and that its activation protects mice from liver injury.

To determine the impact of PPAR $\alpha$  activation on the induction of inflammatory cytokines by D-GalN/LPS-treated ALF, the livers were harvested 6 h after D-GalN/LPS injection. Indeed, PPAR $\alpha$  activation by Wy-14 643 attenuated the expression of proinflammatory cytokines including tumor necrosis factor- $\alpha$  (TNF- $\alpha$ ), interleukin-1 $\beta$  (IL-1 $\beta$ ), IL-6 and IL-12p40. Furthermore, we found that PPAR $\alpha$  activation suppressed the expression of several chemokines, including chemokine (C–C motif) ligand 1 (CCL-1), CCL-2, chemokine (C–X–C motif) ligand-1 (CXCL-1) and CXCL-10, which are important for the recruitment of neutrophils (Figure 2d). We also assayed myeloperoxidase (MPO) activities to measure neutrophil infiltration. As shown in Figure 2e, treatment with Wy-14 643 significantly decreased MPO activity-related injury compared with the D-GalN/LPS insult. Because hepatocyte death is the major cause of ALF, we next measured the impact of the conditioned medium from bone marrow-derived macrophages (BMDMs) stimulated with LPS in the absence or presence of Wy-14 643 on hepatocyte death *in vitro*, with actinomycin D used to mimic the effect of D-GalN. The results showed that conditioned medium of BMDMs stimulated with LPS in the presence of Wy-14 643 led to an increased number of live hepatocytes and lower LDH levels (Figure 2f). These results suggest that the protection of liver injury by PPAR $\alpha$  activation is mediated by reducing inflammation and neutrophil infiltration in the liver in cases of ALF.

NF- $\kappa$ B and mitogen-activated protein kinases (MAPKs) are two of the most important transcription factors in the inflammatory pathways that has major roles in ALF.<sup>28</sup> Thus, we assessed the impact of PPAR $\alpha$  activation on these two pathways. As shown in Figure 2g and Supplementary Figure 2, the phosphorylation levels of NF- $\kappa$ Bp65 were increased by D-GalN/LPS insult and suppressed by Wy-14 643 treatment. In a similar manner, activation of JNK and ERK was also attenuated by Wy-14 643 treatment in the ALF mouse model. Furthermore, we found that the phosphorylation levels of Akt

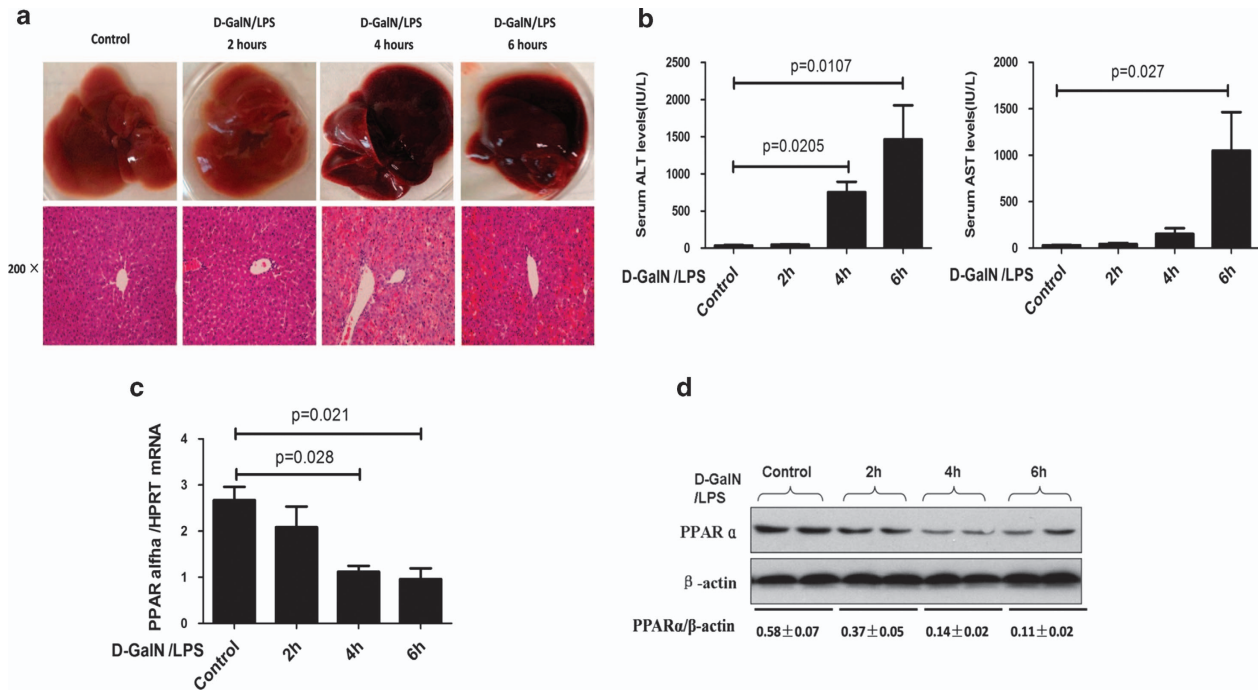


**Figure 1** PPAR $\alpha$  expression is suppressed during ALF progression. Mice were intraperitoneally injected with D-GalN (700 mg/kg) and LPS (10  $\mu$ g/kg) at 2, 4 and 6 h (10 mice per group). The mice in the control group ( $n = 8$ ) were injected with PBS only. (a) Representative livers and H&E staining of livers from the control and the 2-, 4- and 6-h groups. (b) Serum AST and ALT enzyme levels from the control and the 2-, 4- and 6-h groups. (c) Gene expression of PPAR $\alpha$  was measured by qRT-PCR in the livers of the control and the 2-, 4- and 6-h groups. The average target gene/HPRT ratios for each experimental group were plotted. (d) Protein expression levels of PPAR $\alpha$  were measured by western blot assays in the livers of the control and the 2-, 4- and 6-h groups. A representative blot from two samples of every group is shown. Densitometry analysis of the proteins was performed for each sample

is also increased by D-GalN/LPS insult and suppressed by Wy-14643 treatment. These results demonstrated that PPAR $\alpha$  activation-mediated suppression of inflammation is regulated by the NF- $\kappa$ B and MAPK pathways.

**PPAR $\alpha$  activation protects mice from ALF through autophagy mechanisms.** Because a previous study has shown that PPAR $\gamma$  activation induces autophagy in breast cancer cells,<sup>29</sup> we evaluated whether PPAR $\alpha$  activation promotes autophagy pathways in the context of ALF. Quantitative reverse transcription-PCR (qRT-PCR) results showed that, compared with D-GalN/LPS-treated mice, PPAR $\alpha$  activation by Wy-14643 pretreatment in ALF mice promoted the expression of *Atg7* and *Atg5* genes, which are important genes relating to the autophagy pathway, but did not influence *Beclin-1* (Figure 3a). These alterations were confirmed by western blot analyses (Figure 3b and Supplementary Figure 3). Moreover, as shown in Figure 3b and Supplementary Figure 3, PPAR $\alpha$  activation by Wy-14643 pretreatment not only increased the PPAR $\alpha$  expression but also promoted lipidated LC3 form (LC3II) conversion and p62 protein degradation in D-GalN/LPS-induced mice. The results showed that PPAR $\alpha$  activation promotes autophagy during ALF.

Next, we sought to confirm that PPAR $\alpha$  activation leads to the induction of autophagy to protect the liver from injury. First, we applied a specific inhibitor, 3-MA, to block autophagy. Next, we used siRNA to knockdown Atg7. The inhibition of liver Atg7-specific siRNA *in vivo* was confirmed by the

reduced Atg7 levels in the mice (Figure 3c); furthermore, the Atg7 downregulation and 3-MA treatment also decreased the lipidation of LC3I to LC3II (Supplementary Figure 4). The results showed that hepatic protection by Wy-14643 in ALF was completely negated by the inhibition of autophagy, which was evident by the decreased survival (Figure 3e), the significantly higher sALT and sAST levels (Figure 3d), the relatively worse gross morphology and the relatively less preserved liver architecture by histology (Figure 3f). We also verified whether pharmacologic treatment with 3-MA and Atg7 siRNA affects PPAR $\alpha$  expression. The results showed that there were no differences in PPAR $\alpha$  gene expression levels between D-GalN/LPS-treated mice and 3-MA- or Atg7 siRNA-treated mice, but the gene expression of PPAR $\alpha$  is increased in Wy-14643-treated mice (Figure 3g). Autophagic flux in D-GalN/LPS-treated mice was monitored after treatment with Wy-14643 in the presence or absence of chloroquine (CQ). As shown in Figure 3h and Supplementary Figure 5, Wy-14643 pretreatment induced the lipidation of LC3I to LC3II and the degradation of p62 in D-GalN/LPS-induced mice; the CQ pretreatment increased LC3II and p62 accumulation compared with mice treated with Wy-14643 and D-GalN/LPS. Thus, these results demonstrated that hepatoprotective mechanisms of PPAR $\alpha$  activation depend on autophagy pathways.

**PPAR $\alpha$  activation promotes autophagy to suppress the inflammatory response *in vivo*.** Given the ability of PPAR $\alpha$  activation to suppress liver inflammation and promote

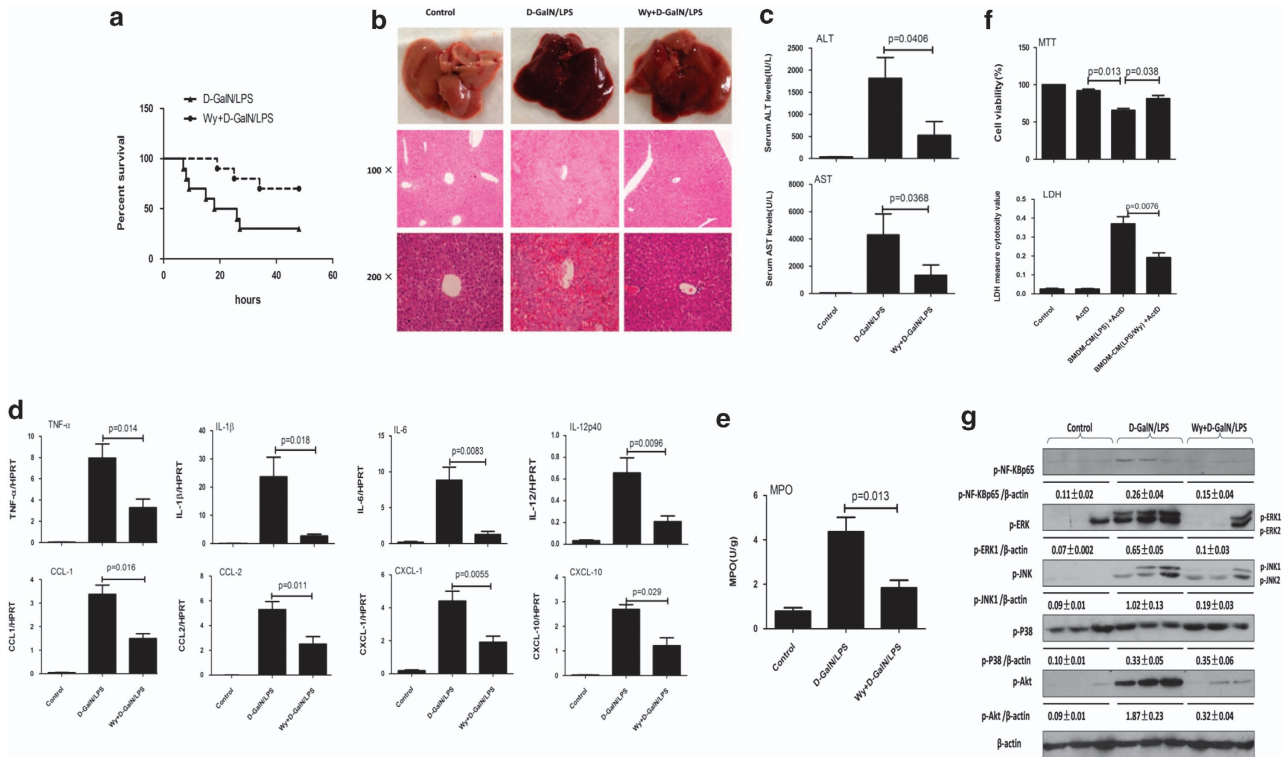


**Figure 2** Wy-14 643 protects against D-GalN/LPS-induced liver injury and suppresses liver inflammation. Wy/D-GalN/LPS-treated mice were administered Wy-14 643 (6 mg/kg) via tail vein injection 2 h before D-GalN/LPS exposure ( $n = 10$ ); D-GalN/LPS-treated mice were pretreated with vehicle (dimethylsulfoxide (DMSO)) 2 h before D-GalN/LPS exposure ( $n = 10$ ). Control mice were pretreated with vehicle (DMSO) 2 h before PBS injection ( $n = 8$ ). The mice were killed 6 h after D-GalN/LPS treatment, and the liver and serum samples were collected (apart from **a**). **(a)** The survival rate of mice was measured in the Wy/D-GalN/LPS-treated group and the D-GalN/LPS-treated group (10 mice per group). **(b)** Representative livers and H&E staining of livers from different groups. **(c)** Serum AST and ALT enzyme levels from different groups. **(d)** Gene expression of TNF- $\alpha$ , IL-1 $\beta$ , IL-6, CCL-1, CCL-2, CXCL-1 and CXCL-10 at 6 h after D-GalN/LPS injection and IL-12p40 at 2 h after D-GalN/LPS injection ( $n = 8$ ). The average target gene/HPRT ratios for each experimental group were plotted. **(e)** Liver MPO levels 6 h after D-GalN/LPS injection. **(f)** BMDMs were stimulated with LPS for 24 h in the absence or presence of Wy-14 643, and then the BMDM-conditioned media were collected. The primary hepatocytes stimulated with actinomycin D in the absence or presence of BMDM-conditioned media for 12 h. The MTT assay and LDH assays were measured. **(g)** The levels of phosphorylated MAP kinases, including JNK, ERK, p38 and phosphorylated NF- $\kappa$ Bp65, phosphorylated Akt and  $\beta$ -actin, were measured by western blotting. A representative blot from three samples of every group is shown. Densitometry analysis of the proteins was performed for each sample

autophagy, we sought to determine whether an autophagy pathway is required for PPAR $\alpha$ -mediated suppression of the inflammatory response. In the context of PPAR $\alpha$  activation in the ALF mice, 3-MA- or Atg7-specific siRNA restored the gene expression of TNF- $\alpha$ , IL-1 $\beta$ , IL-6 and IL-12p40 (Figure 4a). Furthermore, autophagy inhibition increased neutrophil infiltration in mouse livers (Figure 4b) and upregulated the gene expression of chemokines (Figure 4c). These results demonstrated that the autophagy pathways induced by PPAR $\alpha$  activation may contribute to the suppression of liver inflammation in the context of ALF.

**PPAR $\alpha$  activation regulates the primary macrophage TLR4 response *in vitro*.** To further confirm our *in vivo* experimental findings, we investigated the cellular mechanism of the effects of PPAR $\alpha$  activation on macrophages in response to toll-like receptor 4 (TLR4) stimulation by LPS. BMDMs were stimulated by LPS in either the absence or the presence of Wy-14 643 (10, 25 and 50  $\mu$ M). Remarkably, the expression levels of cytokines (Figure 5a) and chemokines (Figure 5b) by LPS-stimulated macrophages were attenuated by Wy-14 643 treatment in a dose-dependent manner. We also measured the PPAR $\alpha$  expression levels in BMDMs

stimulated by LPS in the absence or presence of Wy-14 643 by western blot analysis. As shown in Figure 5c, compared with only LPS treatment, PPAR $\alpha$  expression levels were higher in BMDMs stimulated by LPS in the presence of Wy-14 643. These results indicated that PPAR $\alpha$  activation indeed suppresses the LPS-triggered expression of proinflammatory cytokines and chemokines *in vitro*.

### PPAR $\alpha$ activation suppresses proinflammatory response by promoting autophagy *in vitro*.

We then sought to confirm the role of autophagy *in vitro* in the PPAR $\alpha$ -activated macrophage response. Western blot results showed that Wy-14 643 treatment promoted the expression level of LC3II/I, Atg7, Beclin-1 and Atg5 proteins; meanwhile, Wy-14 643 treatment also increased the degradation of p62 (Figure 6a). Moreover, we transfected the GFP-LC3 plasmid into BMDMs to observe the formation of autophagosomes. As shown in Figure 6b, the GFP-LC3 signal was weak in the control cells, but was bright and punctate after Wy-14 643 treatment, in a dose-dependent manner. To confirm that autophagy induction by Wy-14 643 was exclusively due to PPAR $\alpha$  activation and not to a nonspecific effect of this agonist, we examined the effect of Wy-14 643 treatment on

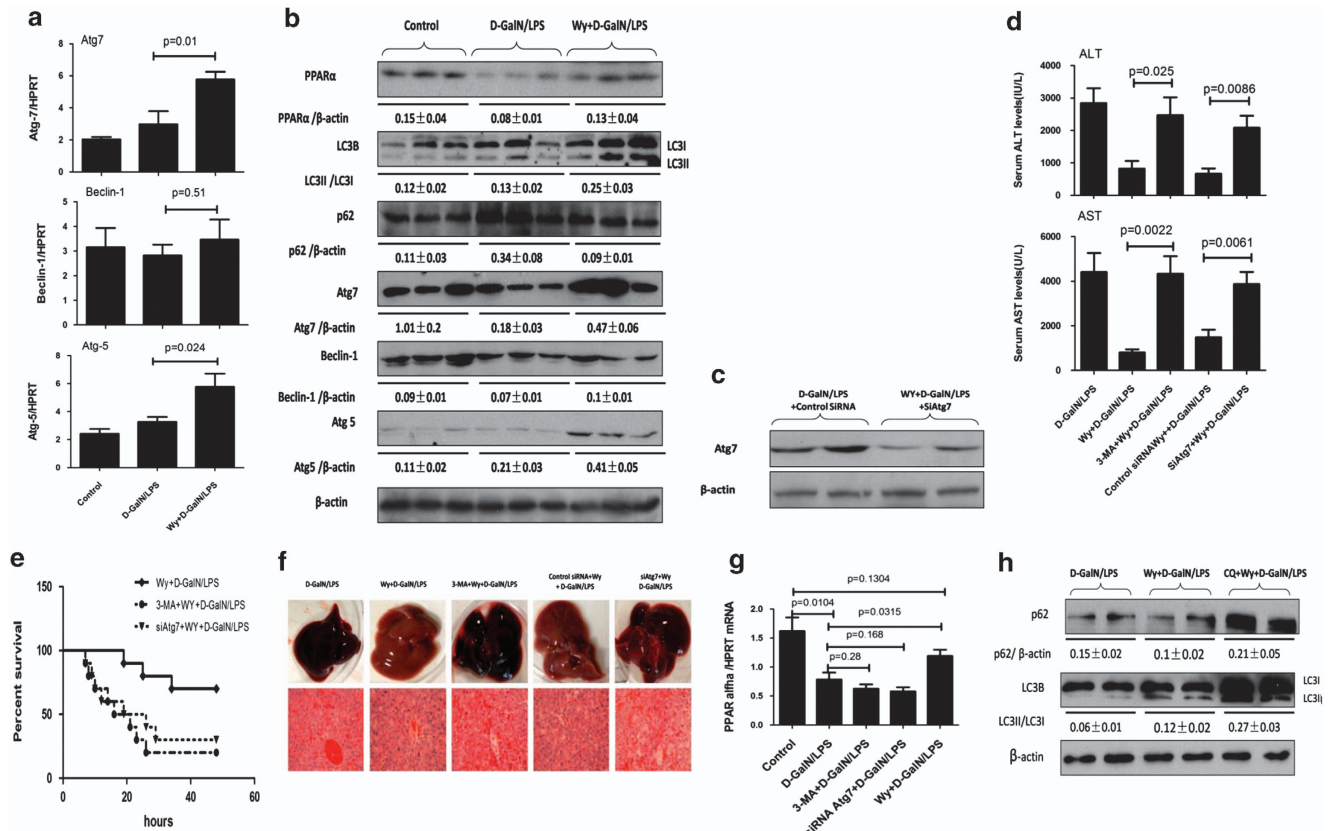


**Figure 3** PPAR $\alpha$  activation protects mice from ALF through autophagy mechanisms. SiAtg7/Wy/D-GalN/LPS-treated mice were pretreated with Atg7 siRNA (50  $\mu$ M/kg) for 48 h via tail vein injection and then administered Wy-14 643 (6 mg/kg) 2 h before D-GalN/LPS exposure ( $n = 8$ ); control siRNA/Wy/D-GalN/LPS-treated mice were pretreated with control siRNA (50  $\mu$ M/kg) for 48 h via tail vein injection, and then administered Wy-14 643 (6 mg/kg) 2 h before D-GalN/LPS exposure ( $n = 9$ ); 3-MA/Wy/D-GalN/LPS-treated mice were coadministered 3-MA (10 mg/kg) and Wy-14 643 at 2 h before D-GalN/LPS exposure ( $n = 7$ ). Mice were killed 6 h after D-GalN/LPS treatment, and liver and serum samples were collected (apart from (d)). (a) Gene expression levels of autophagy-related proteins, including Atg7, Atg5 and Beclin-1, were measured by qRT-PCR in livers from control mice, D-GalN/LPS-treated mice and Wy/D-GalN/LPS-treated mice. The average target gene/HPRT ratios for each experimental group were plotted. (b) Protein expression levels of autophagy-related proteins, including LC3B, Atg7, Atg5, Beclin-1, p62 and PPAR $\alpha$ , were measured by western blotting in livers from control mice, D-GalN/LPS-treated mice and Wy/D-GalN/LPS-treated mice. A representative blot for three samples from each group is shown. Densitometry analysis of the proteins was performed for each sample. (c) Protein expression levels of Atg7 and  $\beta$ -actin were measured by western blotting. A representative blot for two samples from every group is shown. (d) Serum AST and ALT enzyme levels from different groups. (e) The survival rate of mice was measured in different groups (10 mice per group). (f) Representative livers and H&E staining of livers ( $\times 200$ ) from different groups. (g) Gene expression levels of PPAR $\alpha$  were measured by qRT-PCR in control mice ( $n = 8$ ), D-GalN/LPS-treated mice ( $n = 10$ ), siAtg7/D-GalN/LPS-treated mice ( $n = 8$ ), 3-MA/D-GalN/LPS-treated mice ( $n = 9$ ) and Wy-14 643/D-GalN/LPS-treated mice ( $n = 8$ ). (h) Protein expression levels of LC3B, p62 and  $\beta$ -actin were measured by western blotting in livers from D-GalN/LPS-treated mice ( $n = 6$ ), Wy/D-GalN/LPS-treated mice ( $n = 8$ ) and CQ/Wy/D-GalN/LPS-treated mice ( $n = 8$ ). A representative blot for two samples from each group is shown. Densitometry analysis of the proteins was performed for each sample

autophagy-related gene expression using an RNA interference approach to downregulate PPAR $\alpha$  expression in macrophages. As shown in Figure 6c, PPAR $\alpha$  siRNA reduced the Wy-14 643 treatment-induced upregulation of *Atg7*, *Atg5* and *Beclin-1* genes. Furthermore, we tested the effect of Atg7 siRNA or 3-MA treatment in DMEM on autophagy. As shown in Figure 6d, compared with LPS-treated cells, Wy-14 643 treatment increased the ratio of LC3II/I, the expression levels of Atg7 and PPAR $\alpha$ , and also increased the degradation of p62; moreover, compared with Wy-14 643-treated cells, Atg7 siRNA or 3-MA treatment decreased the ratio of LC3II/I, the expression levels of Atg7, decreased the degradation of p62 and almost no change of PPAR $\alpha$ .

Autophagic flux in primary mouse hepatocytes was monitored after treatment with Wy-14 643 in the presence or absence of CQ. The influence of Wy-14 643, with or without CQ, on LC3I/II levels and p62 was assessed by western

blotting. As shown in Figure 6e, Wy-14 643 induced the lipidation of LC3I to LC3II and the degradation of p62. The addition of CQ further increased LC3II conversion, and also decreased the degradation of p62 compared with cells treated with Wy-14 643 only. Taken together, analysis of the level of LC3II/I and p62/ $\beta$ -actin ratio showed that PPAR $\alpha$  activation can directly induce autophagic flux in BMDMs.

To further examine the notion of the PPAR $\alpha$ -mediated autophagy in the macrophages activated by TLR4 signaling, we added 3-MA in Wy-14 643-treated macrophage cultures or transfected siRNA Atg7 into macrophages before Wy-14 643 treatment. Indeed, the LPS-induced proinflammatory cytokine and chemokine levels were restored after inhibition of autophagy (Figures 6f and g). Thus, we concluded that PPAR $\alpha$  activation promotes autophagy to regulate macrophage TLR4 response by downregulating the gene expression of proinflammatory markers and chemokines.

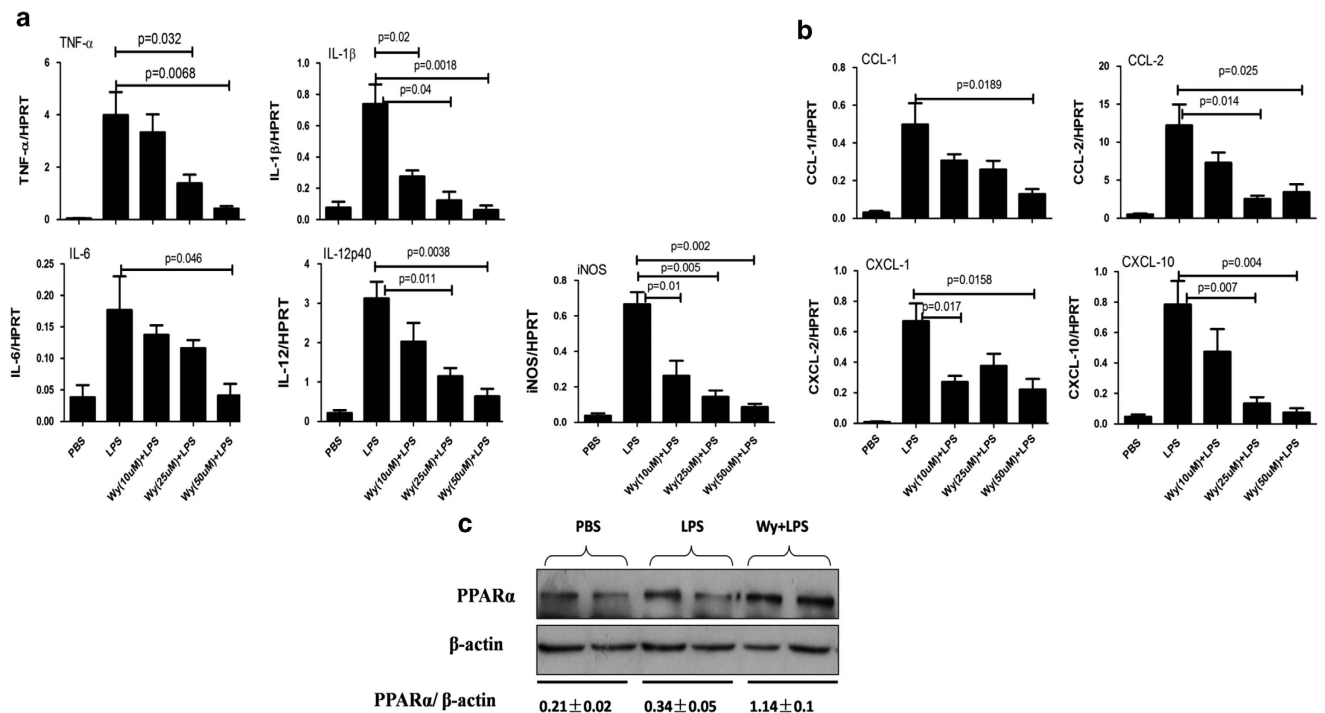
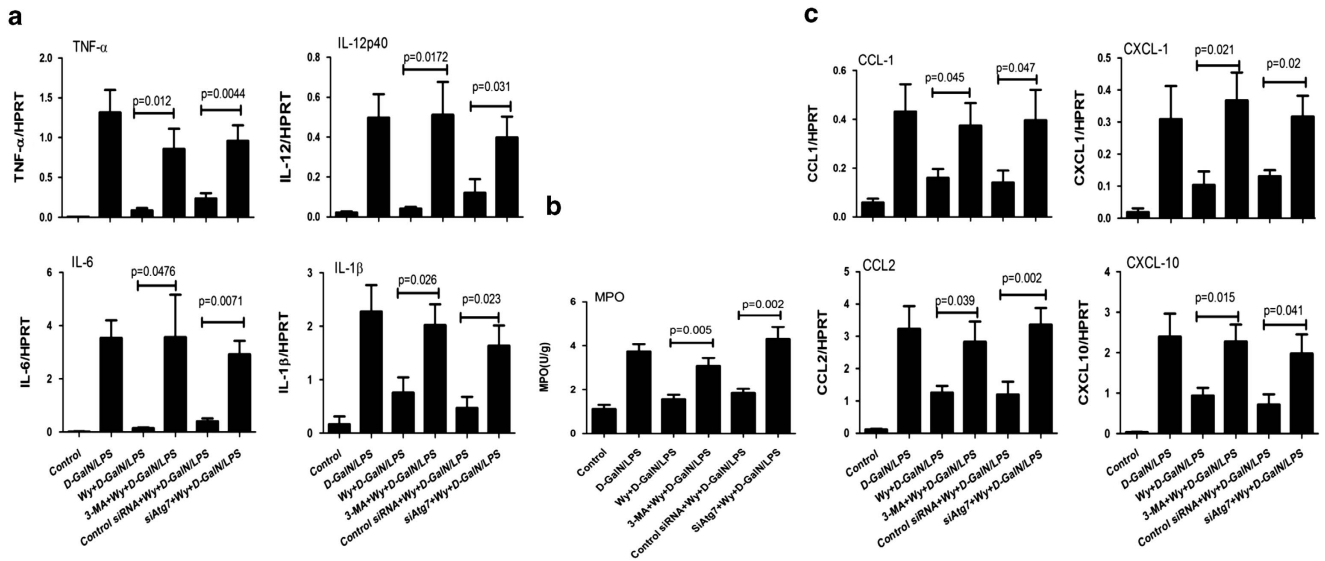


**Figure 5** PPAR $\alpha$  activation regulates the primary macrophage TLR4 response *in vitro*. BMDMs were stimulated with LPS for 1 h (for IL-12p40) or 6 h (for TNF- $\alpha$ , IL-1 $\beta$ , IL-6, inducible nitric oxide synthase (iNOS), CCL-1, CCL-2, CXCL-1 and CXCL-10) in the absence or presence of Wy-14 643 (10, 25 or 50  $\mu$ M). (a) Gene induction of TNF- $\alpha$ , IL-1 $\beta$ , IL-6, IL-12p40 and iNOS was measured by qRT-PCR. The average target gene/HPRT ratios for each experimental group were plotted. (b) Gene induction of CCL-1, CCL-2, CXCL-1 and CXCL-10 was measured by qRT-PCR. The average target gene/HPRT ratios for each experimental group were plotted. (c) Protein expression levels of PPAR $\alpha$  were measured by western blotting in BMDMs stimulated by LPS in the absence or presence of Wy-14 643 (50  $\mu$ M). Densitometry analysis of the proteins was performed

**Decreased expression of PPAR $\alpha$  in the liver of ALF patients with HBV infection.** To determine whether PPAR $\alpha$  participates in the progression of ALF in patients with hepatitis B virus (HBV) infection, we used liver tissues to

measure the changes in PPAR $\alpha$  among normal subjects, chronic hepatitis B (CHB) patients and ALF patients with HBV infection. Relative to the normal controls, the qRT-PCR results showed that PPAR $\alpha$  gene expression levels were not

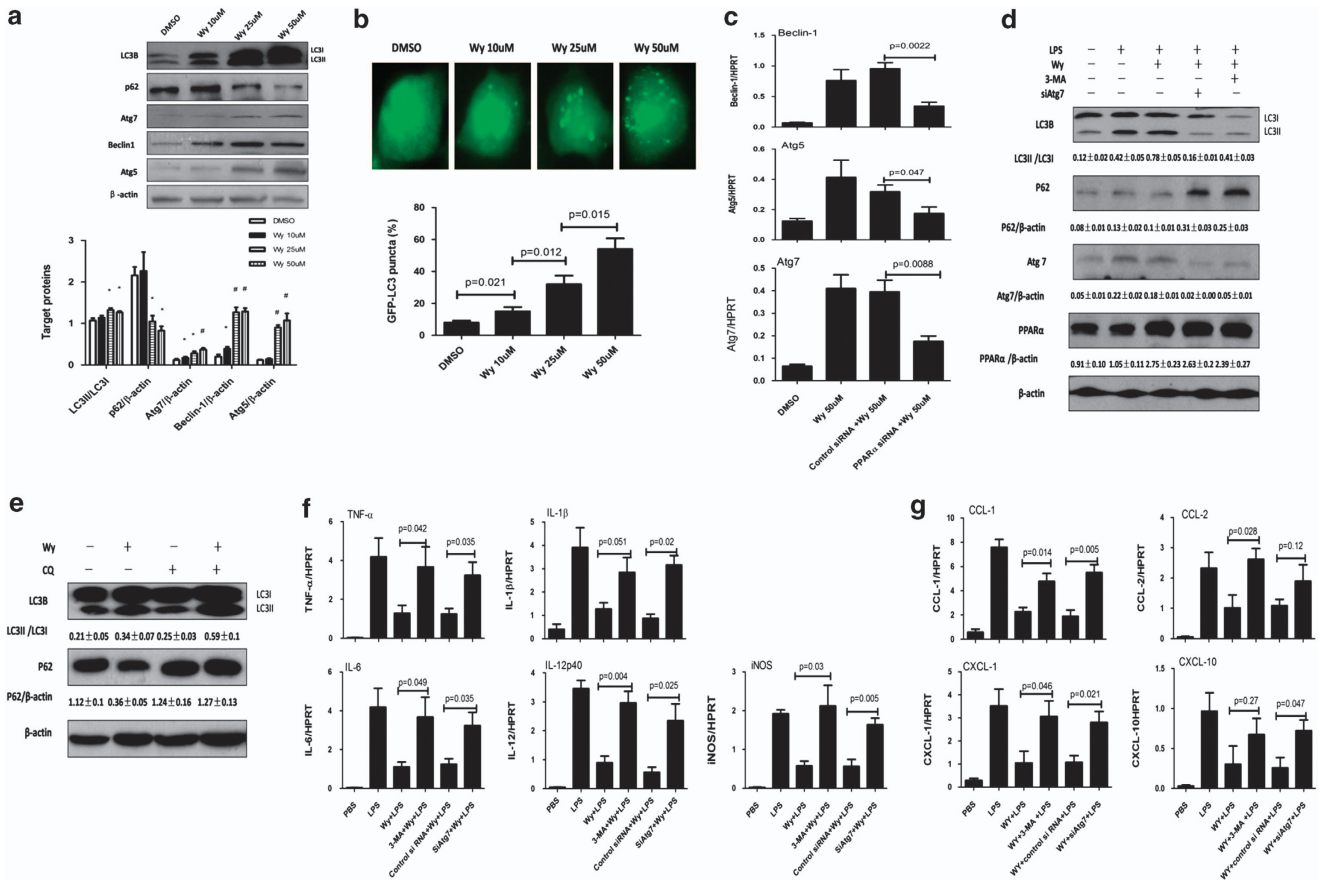


**Figure 6** PPAR $\alpha$  activation suppresses proinflammatory response by promoting autophagy *in vitro*. (a) BMDMs were stimulated with or without Wy-14 643 (10, 25 or 50  $\mu$ M). Total cell lysates were analyzed for LC3B, p62, Atg7, Beclin-1 and Atg5, as well as total  $\beta$ -actin protein levels by western blotting. Densitometry analysis of the proteins was performed for each sample. Data are shown as mean  $\pm$  S.E.M ( $n = 3$ ). \* $P < 0.05$  or # $P < 0.01$ , compared with dimethylsulfoxide (DMSO)-treated BMDMs. (b) Transfected GFP-LC3 plasmid for 12 h, BMDMs were preincubated with Wy-14 643 (10, 25 or 50  $\mu$ M) for 24 h to observe the formation of autophagosomes. The percentage of cells with GFP-LC3 puncta in the groups receiving different concentrations. GFP-positive cells were defined as cells that display bright, punctate staining. Approximately 50 cells were counted, and the experiment was repeated at least three times. (c) After transfection of PPAR $\alpha$  siRNA or control siRNA (3 mg/ml) for 36 h, BMDMs were incubated with or without Wy-14 643 (50  $\mu$ M) for 6 h. Gene induction of Atg7, Atg5 and Beclin-1 was measured by qRT-PCR. The average target gene/HPRT ratios for each experimental group were plotted. (d) After transfection of Atg7 siRNA (3 mg/ml) for 36 h or preincubation with 3-MA (10 mM/l) for 2 h, BMDMs were incubated with or without Wy-14 643 (50  $\mu$ M) for 2 h and then incubated in LPS (20 ng/ml) for 6 h. Western blot analysis shows the LC3BII/I ratio, Atg7, PPAR $\alpha$  and p62 degradation.  $\beta$ -Actin is shown as a loading control; densitometry analysis of the proteins was performed for each sample; data are shown as mean  $\pm$  S.E.M ( $n = 3$ ). (e) Wy-14 643 activates autophagic flux in the primary hepatocytes of mice. Hepatocytes were treated with 50  $\mu$ M Wy-14 643 in the absence or presence of CQ (10  $\mu$ M) for 24 h. Western blot analysis shows the LC3BII/I ratio and p62 degradation.  $\beta$ -Actin is shown as a loading control; densitometry analysis of the proteins was performed for each sample; data are shown as mean  $\pm$  S.E.M ( $n = 3$ ). (f and g) After transfection of Atg7 siRNA (3 mg/ml) for 36 h or preincubated 3-MA (10 mM/l) for 2 h, BMDMs were incubated with or without Wy-14 643 (50  $\mu$ M) for 2 h and then incubated with LPS (20 ng/ml) for 6 h. Cytokine and chemokine gene induction was measured by qRT-PCR. The average target gene/HPRT ratios for each experimental group were plotted

different in the cases of CHB, but were significantly reduced in the cases of ALF (Figure 7a). Similar results were obtained by western blot analyses (Figure 7b) and immunofluorescence staining in liver tissue (Figure 7c). These results indicated that PPAR $\alpha$  expression is also depressed in patients with ALF induced by HBV infection.

## Discussion

Although PPAR $\alpha$  activation exerts strong anti-inflammatory properties in various animal models of liver injury,<sup>30–34</sup> its role in the context of ALF has not yet been explored. The main findings of the present study were that PPAR $\alpha$  activation promotes autophagy, which may depress liver inflammation to

inhibit hepatocyte apoptosis and, consequently, result in liver protection (as depicted in Figure 7d).

Increasing reports in the literature indicate that the systemic inflammatory response, whether through hepatic inflammation and/or sepsis, has a major role in determining the outcome of ALF patients.<sup>35,36</sup> Kupffer cells (macrophages in the liver) not only contribute to the early phase of the disease but also cause sustained inflammation.<sup>37,38</sup> Moreover, immune-mediated liver injury is a consequence of the recruitment of effector leukocytes to the liver where they mediate tissue damage.<sup>39</sup> Leukocyte migration from the vascular lumen into the surrounding extravascular tissue makes a significant contribution to liver injury in ALF.<sup>28,40</sup> Studies have shown that neutrophil accumulation in a liver with ALF can be triggered by a variety of

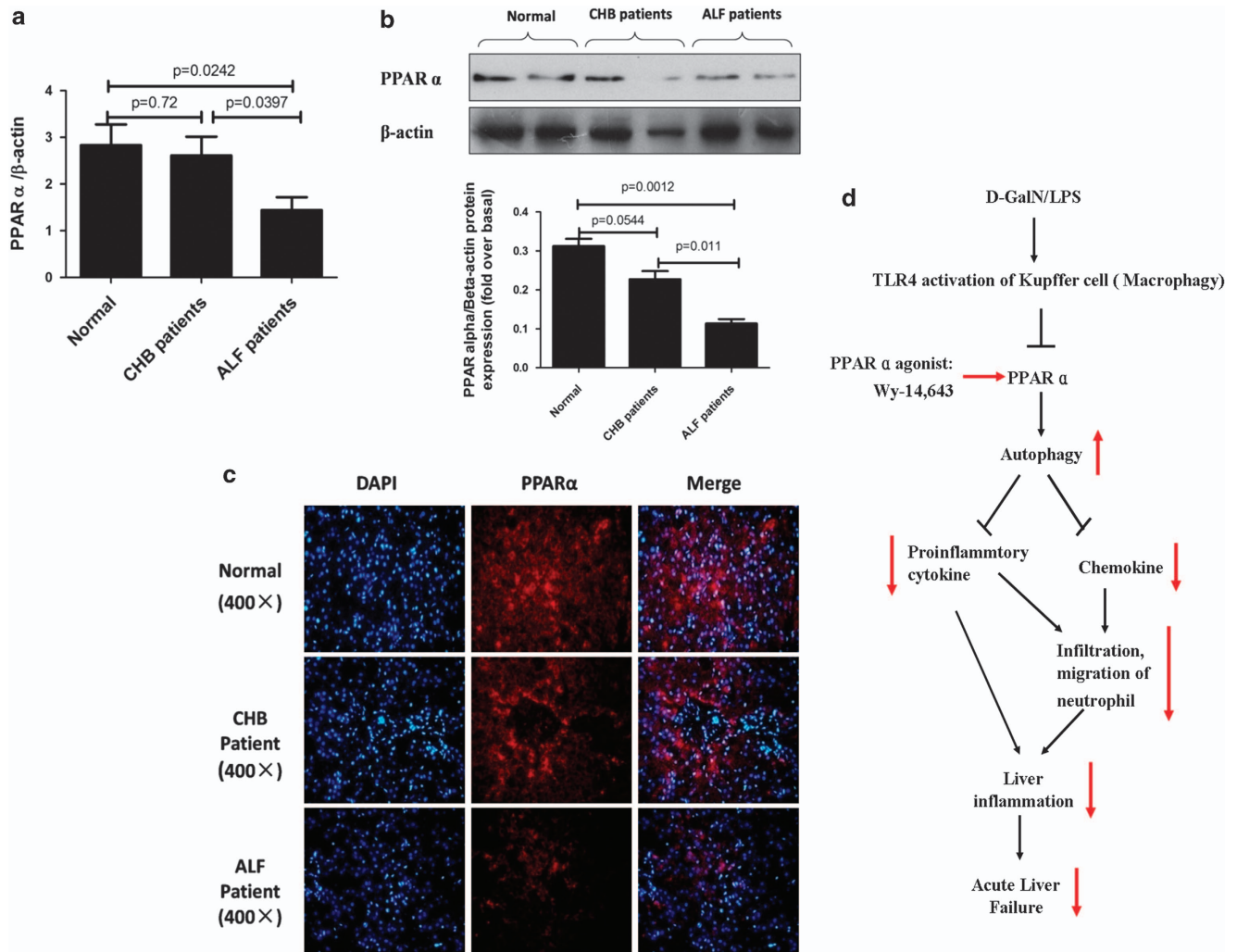


**Figure 7** PPAR $\alpha$  expression is decreased in the liver of ALF patients with HBV infection. (a) Gene expression of PPAR $\alpha$  was measured by qRT-PCR in the livers of normal subjects ( $n=8$ ), CHB patients ( $n=12$ ) and ALF patients ( $n=12$ ). The average target gene/HPRT ratios for each experimental group were plotted. (b) Protein expression levels of PPAR $\alpha$  were measured by western blotting in the livers of normal subjects ( $n=8$ ), CHB patients ( $n=12$ ) and ALF patients ( $n=12$ ). A representative blot from two samples of every group is shown. Densitometry analysis of the proteins was performed for each sample. (c) Immunofluorescence staining for PPAR $\alpha$  (red) in the liver of normal subjects, CHB patients and ALF patients with HBV infection. Representative images of each experiment are shown. Original magnification,  $\times 400$ . (d) In the D-GalN/LPS-induced ALF mice, PPAR $\alpha$  was suppressed, which promotes downregulation of autophagy and increases the expression of proinflammatory cytokines and chemokines. These events lead to incremental neutrophil infiltration and inflammation in the liver and ultimately induce the development of ALF. Red arrows indicate PPAR $\alpha$  agonist; Wy-14 643 induced changes in ALF mice relative to their DMSO-injected counterparts

proinflammatory mediators and chemokines.<sup>41,42</sup> Our results showed that PPAR $\alpha$  activation significantly reduced the D-GalN/LPS-induced acute liver damage by reducing the expression of proinflammatory cytokines and chemokines, regulating the activities of the NF- $\kappa$ B and MAPK pathways. Therefore, we speculate that one of the protective mechanisms of PPAR $\alpha$  activation is the reduced activation of the NF- $\kappa$ B and MAPK pathways in the liver in cases of ALF. In one regard, this mechanism can repress the cascade activation of inflammatory cytokines and directly control liver inflammation. By contrast, PPAR $\alpha$  activation significantly decreased the expression of chemokines, which resulted in mitigating neutrophil migration and infiltration in the liver, further indirectly alleviating inflammation. Taken together, our results confirmed that PPAR $\alpha$  activation can effectively treat liver injury due to ALF. This finding

implicates PPAR $\alpha$  as an important target for the effective intervention of ALF.

What is the underlying mechanism mediating the effect of PPAR $\alpha$  activation on liver inflammation? The regulation of autophagy via PPAR $\alpha$  signaling is a novel finding. Autophagy is an intracellular degradation process through which long-lived cytosolic proteins and organelles are degraded by lysosomes and recycled. Autophagic flux can be monitored by combining the measurement of LC3II and p62 levels. An increase of LC3II conversion with the degradation of p62 indicates the induction of autophagic flux, whereas the increase of LC3II conversion without the degradation of p62 indicates the inhibition of autophagic flux.<sup>42</sup> Our results demonstrated that PPAR $\alpha$  activation can upregulate the autophagy-related genes *Atg5* and *Atg7*; more importantly, PPAR $\alpha$  activation increase LC3II



conversion and p62 degradation *in vivo* and *in vitro*. In conclusion, our study revealed that PPAR $\alpha$  activation promotes autophagic flux in the progression of D-GalN/LPS-induced ALF.

Because autophagy affects the effector cells of innate and adaptive immunity, which mediate the inflammatory response, its activity in these cells influences the anti-microbial response, and the development of an effective cognate immune defense. Loss or decreased autophagy may lead to necrotic death that can initiate an inflammatory reaction in phagocytes through their surface and cytosolic receptors; thus, autophagy can shape inflammatory responses.<sup>43</sup> Our preliminary research found that autophagy is promoted in the early phase of D-GalN/LPS-induced ALF and inhibited in the later phase of D-GalN/LPS-induced ALF, and it has a protective role in ALF (Ren Feng *et al.*, unpublished paper). We further explored the role of autophagy in the protection of PPAR $\alpha$  activation-treated ALF. We found that inhibition of autophagy reversed the protective effect of PPAR $\alpha$  activation on ALF, restored the upregulation of gene expression of the inflammatory cytokines and chemokines and reversed the decreased infiltration and migration of neutrophils in the liver. We demonstrated a new pathogenic mechanism of ALF that PPAR $\alpha$  activation attenuates the inflammatory response to protect against D-GalN/LPS-induced ALF in mice by promoting autophagy.

A previous study demonstrated that reductions in PPAR $\alpha$  levels resulted in a significant inhibition of HBV replication in HepG2 cells.<sup>44</sup> However, the role of PPAR $\alpha$  expression in the progression of ALF patients with HBV infection remains unclear. Our studies further explored this role and showed that PPAR $\alpha$  levels are not influenced in CHB patients compared with normal subjects, whereas it is downregulated in ALF patients with HBV infection. It can be speculated that PPAR $\alpha$  may have an important role in the pathogenesis of HBV infection-induced ALF, especially in the regulation of liver inflammation; however, the mechanisms may differ between mouse ALF induced by D-GalN/LPS and human ALF induced by HBV. Based on our findings, we speculate that PPAR $\alpha$  levels can be considered an early warning sign of ALF with HBV infection. Additional in-depth research for these questions is needed.

A limitation of our study is that we could not assess exactly how PPAR $\alpha$  regulates the autophagy pathway. We have found that PPAR $\alpha$  activation significantly inhibits the phosphorylation levels of Akt in D-GalN/LPS-induced ALF, and previous studies have shown that activation of the PI3K-Akt pathway significantly inhibits the autophagic pathway.<sup>45,46</sup> Therefore, we hypothesize that PPAR $\alpha$  activation may regulate autophagy through the PI3K-Akt pathway signaling pathway in the progression of ALF. At present, this hypothesis is under further exploration.

In summary, this study adds to the general understanding of mechanisms of ALF and provides new insight into the importance of PPAR $\alpha$  in regulating liver inflammation, partially through an autophagy pathway. Therefore, PPAR $\alpha$  activation represents a potent strategy to ameliorate ALF pathology. Further preclinical studies on PPAR $\alpha$  agonists are warranted for the development of a clinically applicable therapeutic strategy against ALF.

## Materials and Methods

**Animal experiments.** Male wild-type (C57BL/6) mice (aged 8–12 weeks) were purchased from Capital Medical University (Beijing, China) and housed in the Capital Medical University animal facility under specific pathogen-free condition and received humane care according to Capital Medical University Animal Care Committee guidelines.

The mice were intraperitoneally injected with D-GalN (700 mg/kg; Sigma, St. Louis, MO, USA) and LPS (10  $\mu$ g/kg; InvivoGen, San Diego, CA, USA) to induce ALF or with saline in the control animals. The PPAR $\alpha$  activator Wy-14 643 (6 mg/kg; Sigma) was administered via injection into the tail vein 2 h before D-GalN/LPS exposure. Suppression of autophagy was achieved by tail vein injection of 3-MA (10 mg/kg; Sigma) or siRNA for Atg7 (50  $\mu$ M/kg). CQ (C6628; Sigma-Aldrich, St. Louis, MO, USA) was dissolved in normal saline solution. Mice were pre-treated with CQ (50 mg/kg, intraperitoneally) 2 h before D-GalN/LPS exposure. The mice were killed at various time points after D-GalN/LPS treatment, and liver and serum samples were collected for future analysis.

**Human specimens.** Normal liver samples were collected from eight patients undergoing hepatic resection for liver transplantation. CHB samples were obtained from the livers of 12 patients undergoing liver puncture biopsy. ALF samples were obtained from the livers of 12 patients with HBV infection undergoing liver transplantation. This study meets the ethical guidelines of the 1975 Declaration of Helsinki, and the study protocol was approved by the Medical Ethics Committee of Beijing YouAn Hospital. Informed consent was obtained from all patients. The clinical characteristics and details of the patients included in the study are shown in Table 1.

## Hepatocellular damage assay, liver histology and MPO assay.

Serum aminotransferase, liver histology by H&E staining and MPO assays were performed as described previously.<sup>47,48</sup>

**Quantitative real-time PCR analysis and primer sequences.** Total RNA was isolated from hepatic samples using Trizol reagent according to the manufacturer's protocol. A total of 2.5  $\mu$ g of RNA was reverse transcribed into cDNA using SuperScript III First-Strand Synthesis System (Invitrogen, Carlsbad, CA, USA). Quantitative PCR was performed using the DNA Engine with Chromo 4 Detector (MJ Research, Waltham, MA, USA). The following were added to a final reaction volume of 20  $\mu$ l: 1  $\times$  SuperMix (Platinum SYBR Green qPCR Kit; Invitrogen); cDNA (2  $\mu$ l); and 0.5  $\mu$ M of each primer. The amplification conditions were as follows: 50  $^{\circ}$ C for 2 min and 95  $^{\circ}$ C for 5 min, followed by 50 cycles of 95  $^{\circ}$ C for 15 s and 60  $^{\circ}$ C for 30 s. The primers used to amplify the specific mouse gene fragments are listed in Table 2.

**Western blot analyses.** Protein was extracted from liver tissue in RIPA buffer together with phosphatase and protease inhibitors. Proteins in SDS-loading buffer were subjected to SDS-12% polyacrylamide gel electrophoresis and transferred to a PVDF membrane (Bio-Rad, Hercules, CA, USA). Antibodies against PPAR $\alpha$  (Abcam, Cambridge, MA, USA), phosphorylated ERK, phosphorylated JNK, phosphorylated p38, phosphorylated NF- $\kappa$ Bp65, LC3B, Atg7, Atg5, Beclin-1, Lamp1 and  $\beta$ -actin (Cell Signaling Technology Inc., Santa Cruz, CA, USA) were used for western blot analysis. The membranes were probed with primary antibodies (1:500–1000) in 10 ml of blocking buffer overnight at 4  $^{\circ}$ C. After washing, the membranes were further probed with the appropriate horseradish peroxidase-conjugated secondary antibody (1:2000) in 10 ml of blocking buffer for 1 h at room temperature. SuperSignal West Pico chemiluminescent substrates (Thermo Fisher Scientific, Rockford, IL, USA) were used for chemiluminescence development.

**Atg7 siRNA treatment *in vivo*.** Autophagy was inhibited through the siRNA against Atg7 (50  $\mu$ M/kg; Jima, Suzhou, China); its sequence is 5'-GCAUCAUCUUGCAAGUGAATT-3'. Atg7 knockdown was achieved by siRNA using an Entranster *in vivo* transfection reagent (Engreen Biosystem Co., Beijing, China) via hydrodynamic tail vein injection in mice. Scrambled siRNA (50  $\mu$ M/kg) was used as a control. The processes were performed following the manufacturer's instructions.

**BMDM cell culture and treatment.** Murine BMDMs, differentiated from bone marrow cells, were prepared by culturing cells in DMEM containing 10% fetal bovine serum, 1% penicillin/streptomycin and 20% L929 conditioned medium

**Table 1** General clinical characteristics of the different study groups

	Normal subjects (n = 8)	Chronic hepatitis B patients (n = 12)	Acute liver failure patients (n = 12)	P-value
Age (years)	39.4 ± 3.6	32.4 ± 4.1	41.6 ± 5.3	0.11
Gender (male/female)	6/2	7/5	8/4	0.437
Alanine aminotransferase (U/l)	35.1 ± 6.1	93.3 ± 18.3	210.4 ± 76.3	0.026
Aspartate aminotransferase (U/l)	30.6 ± 3.9	62.6 ± 15.4	305.8 ± 44.6	0.038
Serum bilirubin ( $\mu$ mol/l)	8.8 ± 2.9	20.9 ± 6.3	196.1 ± 50.6	0.01
Prothrombin time (s)	9 ± 2.4	15 ± 5.2	34.4 ± 7.2	0.022
Albumin (g/l)	46.2 ± 6.9	32.6 ± 10.8	26.7 ± 5.7	0.039
Creatinine ( $\mu$ mol/l)	73.6 ± 21.5	80.1 ± 29.0	95.4 ± 32.8	0.042
Hepatic encephalopathy score	—	—	1.7 ± 0.3	—
Child–Pugh score	—	6 ± 0.6	13.7 ± 2.4	0.031
Model for end-stage liver disease score	—	—	28.2 ± 4.2	—
HBsAg test	—	Positive	Positive	—

**Table 2** Sequences of the primers for SYBR Green real-time RT-PCR

Target gene	Forward primers	Reverse primers
<i>HPRT</i>	5'-TCAACGGGGGACATAAAAAGT-3'	5'-TGCATTGTTTTACCAGTGTCAA-3'
<i>TNF-<math>\alpha</math></i>	5'-GCCTCTTCTCATTCCGCTTGT-3'	5'-TTGAGATCCATGCCGTTG-3'
<i>IL-1<math>\beta</math></i>	5'-TTGACGGACCCAAAAGAT-3'	5'-GATGATCTGAGGTGTGAGGGTCTG-3'
<i>IL-6</i>	5'-GCTACCAAAGTGGATATAATCAGGA-3'	5'-CCAGGTAGCTATGGTACTCCAGAA-3'
<i>IL-12p40</i>	5'-CAGCTTCTTCATCAGGGACAT-3'	5'-CTTGAGGGAGAAGTAGGAATGG-3'
<i>iNOS</i>	5'-CACCTTGAGTTCACCCAGT-3'	5'-ACCACTCGTACTTGGGATGC-3'
<i>CCL-1</i>	5'-GTACCTGAACCGCATCTG-3'	5'-GCTGAGCAGGGTCTTCAGAG-3'
<i>CCL-2</i>	5'-TGACCACCTAGAGCCTTGG-3'	5'-TGTTCCCGTAGAGATCCACAA-3'
<i>CXCL1</i>	5'-ACTTCAAGAATCCAGAG-3'	5'-CTTCCAGGTGAGTTCAGC-3'
<i>CXCL10</i>	5'-GCTGCCGTCATTTTCTGC-3'	5'-TCTCACTGGCCGTCATC-3'
<i>Atg7</i>	5'-TCCGTTGAAGTCTCTGCTT-3'	5'-CCACTGAGGTTCCACCATCCT-3'
<i>Atg5</i>	5'-AGATGGACAGCTGCACACAC-3'	5'-GCTGGGGGACAATGCTAATA-3'
<i>Beclin-1</i>	5'-GGCCAATAAGATGGGTCTGA-3'	5'-GCTGCACACAGTCCAGAAAA-3'
<i>Lamp1</i>	5'-GATGAATGCCAGCTTAGCC-3'	5'-CTGACCTGCACACTGAAGA-3'

for 6 days. LPS (20 ng/ml) was used to activate cells, Wy-14643 (50  $\mu$ M) was used to activate PPAR $\alpha$ , siRNA PPAR $\alpha$  (5'-GAGAUCGGCCUGGCCUUAUAAA-CAU-3') was used to inhibit PPAR $\alpha$  and 3-MA (10 mM) or Atg7 siRNA (3 mg/ml) was used to inhibit autophagy in the macrophages. Transient transfection was performed with a GFP-LC3 plasmid or Atg7 siRNA using Fugene HD (Roche, Shanghai, China) according to the manufacturer's instructions.

For macrophage-conditioned media, BMDMs were seeded in six-well plates at a density of  $4 \times 10^6$  cells per well in 3 ml of complete medium and incubated for 12 h. BMDMs were stimulated with LPS (20 ng/ml) in the absence or presence of Wy-14643 (50  $\mu$ M) for 24 h. The BMDM-conditioned media were collected, clarified by centrifugation at  $400 \times g$  and stored at  $-20^\circ\text{C}$  until use.

**Isolation and treatment of primary mouse hepatocytes.** The mouse livers were perfused with Hank's solution containing collagenase at 7 weeks of age, and viable hepatocytes were isolated by Percoll isodensity centrifugation as described.<sup>49</sup> The primary hepatocytes stimulated with actinomycin D (1  $\mu$ g/ml; Sigma) in the absence or presence of BMDM-conditioned media for 12 h. The MTT assay (Amersco, Solon, OH, USA) was used as a qualitative index of cell proliferation, and apoptosis was evaluated at 12 h by LDH assays (Biochain Institute, Hayward, CA, USA). The processing was conducted according to the manufacturer's instructions.

**Immunofluorescence staining.** Paraffin sections were treated with xylene for 10 min three times. The sections were hydrated through a graded alcohol series and then rinsed three times with distilled water. The slides were incubated for 20 min in 10% goat serum in PBS and then a PPAR $\alpha$  rabbit polyclonal antibody (Abcam) overnight at  $4^\circ\text{C}$ . The slides were incubated with Alexa Fluor 568 goat anti-rabbit IgG (1:200; Invitrogen, Grand Island, NY, USA) for 45 min. After three washes with PBS, the nuclei were stained with 4',6-diamidino-2-phenylindole (1  $\mu$ g/ml; Shizebio, Shanghai, China) for 10 min. The images were examined on a Nikon Eclipse E800 fluorescent microscope (Nikon Corp., Tokyo, Japan).

**Statistical analyses.** The results are shown as the mean  $\pm$  S.E.M. The statistical analyses were performed using an unpaired Student's *t*-test, and  $P < 0.05$  (two tailed) was considered significant.

### Conflict of Interest

The authors declare no conflict of interest.

**Acknowledgements.** This work was financially supported by China National Key Project of the Twelfth Five-year Plan (2012ZX10002004-006, 2012ZX10004904-003-001 and 2013ZX10002002-006-001), the National Natural Science Foundation of China (81270532, 81372094 and 81300349), the Beijing Excellent Talents Training Funding (2011D003034000022), the Technology Foundation for Selected Overseas Chinese Scholar, Ministry of Personnel of Beijing (2012) and Applied Research for the Clinical Characteristics of Capital (Z121107001012167).

1. Hoofnagle JH, Carithers RJ, Shapiro C, Ascher N. Acute hepatic failure: summary of a workshop. *Hepatology* 1995; **21**: 240–252.
2. Riordan SM, Williams R. Mechanisms of hepatocyte injury, multiorgan failure, and prognostic criteria in acute liver failure. *Semin Liver Dis* 2003; **23**: 203–215.
3. Desvergne B, Wahli W. Peroxisome proliferator-activated receptors: nuclear control of metabolism. *Endocr Rev* 1999; **20**: 649–688.
4. Kota BP, Huang TH, Roufogalis BD. An overview on biological mechanisms of PPARs. *Pharmacol Res* 2005; **51**: 85–94.
5. Staels B, Dallongeville J, Auwerx J, Schoonjans K, Leitersdorf E, Fruchart JC. Mechanism of action of fibrates on lipid and lipoprotein metabolism. *Circulation* 1998; **98**: 2088–2093.
6. Chinetti G, Griglio S, Antonucci M, Pineda TI, Delerive P, Majd Z *et al*. Activation of peroxisome proliferator activated receptors  $\alpha$  and  $\gamma$  induces apoptosis of human monocyte derived macrophages. *J Biol Chem* 1998; **273**: 25573–25580.

7. Delerive P, De BK, Besnard S, Vanden BW, Peters JM, Gonzalez FJ *et al*. PPAR $\alpha$  negatively regulates the vascular inflammatory gene response by negative cross talk with transcription factors NF- $\kappa$ B and AP-1. *J Biol Chem* 1999; **274**: 32048–32054.
8. Devchand PR, Keller H, Peters JM, Vasquez M, Gonzalez FJ, Wahli W. The PPAR $\alpha$ -leukotriene B pathway to inflammation control. *Nature* 1996; **384**: 39–43.
9. Staels B, Koenig W, Habib A, Merval R, Lebret M, Pineda-Torra I *et al*. Activation of human aortic smooth-muscle cells is inhibited by PPAR $\alpha$  but not by PPAR $\gamma$  activators. *Nature* 1998; **393**: 790–793.
10. Lee JH, Joe EH, Jou I. PPAR-alpha activators suppress STAT1 inflammatory signaling in lipopolysaccharide-activated rat glia. *NeuroReport* 2005; **16**: 829–833.
11. Delayre OC, Becker J, Guenon I, Lagente V, Auwerx J, Frossard N *et al*. PPARalpha downregulates airway inflammation induced by lipopolysaccharide in the mouse. *Respir Res* 2005; **6**: 91–100.
12. Di PR, Esposito E, Mazzon E, Genovese T, Muia C, Crisafulli C *et al*. Absence of peroxisome proliferators-activated receptors (PPAR)alpha enhanced the multiple organ failure induced by zymosan. *Shock* 2006; **26**: 477–484.
13. Sheu MY, Fowler AJ, Kao J, Schmutz M, Schoonjans K, Auwerx J *et al*. Topical peroxisome proliferator activated receptor-alpha activators reduce inflammation in irritant and allergic contact dermatitis models. *J Invest Dermatol* 2002; **118**: 94–101.
14. Seong HY, Mohamed AA, Byoung JS. Activation of PPARa by Wy-14,643 ameliorates systemic lipopolysaccharide-induced acute lung injury. *Biochem Biophys Res Commun* 2013; **9**: 0006-291X(13)00870-X.
15. Stephen WS, Charles CC, Basilia Z, Hector RW. Reduced peroxisome proliferator-activated receptor  $\alpha$  expression is associated with decreased survival and increased tissue bacterial load in sepsis. *Shock* 2012; **37**: 164–169.
16. Seong HY, Ogyi P, Lauren EH, Mohamed AA, Kwan HM, Byoung JS. Lack of PPAR $\alpha$  exacerbates lipopolysaccharide-induced liver toxicity through STAT1 inflammatory signaling and increased oxidative/nitrosative stress. *Toxicol Lett* 2011; **202**: 23–29.
17. Mignon A, Rouquet N, Fabre M, Martin S, Pagès JC, Dhainaut JF *et al*. LPS challenge in D-galactosamine-sensitized mice accounts for caspase-dependent fulminant hepatitis, not for septic shock. *Am J Respir Crit Care Med* 1999; **159**: 1308–1315.
18. Nakama T, Hirano S, Moriuchi A, Hasuike S, Nagata K, Hori T *et al*. Etoposide prevents apoptosis in mouse liver with D-GalN/LPS-induced fulminant hepatic failure resulting in reduction of lethality. *Hepatology* 2001; **33**: 1441–1450.
19. Ohsumi Y. Molecular dissection of autophagy: two ubiquitin-like systems. *Nat Rev Mol Cell Biol* 2001; **2**: 211–216.
20. Mizushima N, Levine B, Cuervo AM, Klionsky DJ. Autophagy fights disease through cellular self-digestion. *Nature* 2008; **451**: 1069–1075.
21. Levine B, Deretic V. Unveiling the roles of autophagy in innate and adaptive immunity. *Nat Rev Immunol* 2007; **7**: 767–777.
22. Beth L, Noboru M, Herbert WV. Autophagy in immunity and inflammation. *Nature* 2011; **469**: 323–335.
23. Alexander JSC, Stefan WR. Autophagy in inflammatory diseases. *Int J Cell Biol* 2011; **2011**: 732798.
24. Delgado MA, Elmaoued RA, Davis AS, Kyei G, Deretic V. Toll-like receptors control autophagy. *EMBO J* 2008; **27**: 1110–1121.
25. Xu Y, Jagannath C, Liu XD, Sharafkhaneh A, Kolodziejaska KE, Eissa NT. Toll-like receptor 4 is a sensor for autophagy associated with innate immunity. *Immunity* 2007; **27**: 135–144.
26. Saitoh T, Fujita N, Jang MH, Uematsu S, Yang BG, Satoh T *et al*. loss of the autophagy protein Atg16L1 enhances endotoxin-induced IL-1 $\beta$  production. *Nature* 2008; **456**: 264–268.
27. Nakahira K, Haspel JA, Rathinam VA, Lee SJ, Dolinay T, Lam HC *et al*. Autophagy proteins regulate innate immune responses by inhibiting the release of mitochondrial DNA mediated by the NALP3 inflammasome. *Nat Immunol* 2011; **12**: 222–230.
28. Gyongyi S, Pranoti M, Angela D. Innate immune response and hepatic inflammation. *Semin Liver Dis* 2007; **27**: 339–350.
29. Jie Z, Zh Wei, Bing L, Mathew CC, Diana WM, Min W *et al*. PPAR $\gamma$  activation induces autophagy in breast cancer cells. *Int J Biochem Cell Biol* 2009; **41**: 2334–2342.
30. Delayre OC, Becker J, Guenon I, Lagente V, Auwerx J, Frossard N *et al*. PPAR $\alpha$  downregulates airway inflammation induced by lipopolysaccharide in the mouse. *Respir Res* 2005; **6**: 91–100.
31. Nakajima T, Kamijo Y, Tanaka N, Sugiyama E, Tanaka E, Kiyosawa K *et al*. Peroxisome proliferator-activated receptor  $\alpha$  protects against alcohol-induced liver damage. *Hepatology* 2004; **40**: 972–980.
32. Nan YM, Kong LB, Ren WG, Wang RQ, Du JH, Li WC *et al*. Activation of peroxisome proliferator activated receptor alpha ameliorates ethanol mediated liver fibrosis in mice. *Lipids Health Dis* 2013; **12**: 11–20.
33. Seong HY, Ogyi P, Lauren EH, Mohamed AA, Kwan HM, Byoung JS. Lack of PPAR $\alpha$  exacerbates lipopolysaccharide-induced liver toxicity through STAT1 inflammatory signaling and increased oxidative/nitrosative stress. *Toxicol Lett* 2011; **202**: 23–29.
34. Emilia I, Geoff F, Pauline H, Graham R, Isabelle L. Administration of the potent PPAR $\alpha$  Agonist, Wy-14,643, reverses nutritional fibrosis and steatohepatitis in mice. *Hepatology* 2004; **39**: 1286–1296.
35. Rolando N, Wade J, Davalos M, Wendon J, Philpott-Howard J, Williams R. The systemic inflammatory response syndrome in acute liver failure. *Hepatology* 2000; **32**: 734–739.
36. Jalan R, Olde Damink SW, Hayes PC, Deutz NE, Lee A. Pathogenesis of intracranial hypertension in acute liver failure: inflammation, ammonia and cerebral blood flow. *J Hepatol* 2004; **41**: 613–620.
37. Su GL. Lipopolysaccharides in liver injury: molecular mechanisms of kupffer cell activation. *Am J Physiol Gastrointest Liver Physiol* 2002; **283**: G256–G265.
38. Matsuno K, Nomiya H, Yoneyama H, Uwatoku R. Kupffer cell-mediated recruitment of dendritic cells to the liver crucial for a host defense. *Dev Immunol* 2002; **9**: 143–149.
39. Klugewitz K, Adams DH, Emoto M, Eulenburg K, Hamann A. The composition of intrahepatic lymphocytes: shaped by selective recruitment? *Trends Immunol* 2004; **25**: 590–594.
40. Bertus E, Simon CA, Stephen JW, Andrew PH, David HA. Immune-mediated liver injury. *Semin Liver Dis* 2007; **27**: 351–366.
41. Wagner JG, Roth RA. Neutrophil migration during endotoxemia. *J Leukoc Biol* 1999; **66**: 10–24.
42. Klionsky DJ, Abdalla FC, Abeliovich H, Abraham RT, Acevedo A, Adeli K *et al*. Guidelines for the use and interpretation of assays for monitoring autophagy. *Autophagy* 2012; **8**: 445–544.
43. Fésüs L, Demény MÁ, Petrovski G. Autophagy shapes inflammation. *Antioxid Redox Signal* 2011; **14**: 2233–2243.
44. Hu W, Wang X, Ding X, Li Y, Zhang X, Xie P *et al*. MicroRNA-141 represses HBV replication by targeting PPAR $\alpha$ . *PLoS One* 2012; **7**: e34165.
45. Wu YT, Tan HL, Huang Q, Ong CN, Shen HM. Activation of the PI3K-Akt-mTOR signaling pathway promotes necrotic cell death via suppression of autophagy. *Autophagy* 2009; **5**: 824–834.
46. Sovan S, Janet ED, Marie F, Moises GA, Zeyn GT, Maria JS *et al*. Regulation of mammalian autophagy in physiology and pathophysiology. *Physiol Rev* 2010; **90**: 1383–1435.
47. Liyan C, Feng R, Haiyan Z, Tao W, Zhengfu P, Li Z *et al*. Inhibition of GSK3 $\beta$  ameliorates D-GalN/LPS-induced liver injury by reducing ERS-triggered apoptosis. *PLoS One* 2012; **7**: e45202.
48. Feng R, Zhongping D, Xiuda S, Shen X, Gao F, Bai L *et al*. The inhibition of GSK3 $\beta$  ameliorates liver ischemia reperfusion injury via an IL-10-mediated immune modulatory mechanism. *Hepatology* 2011; **54**: 687–696.
49. Klauunig JE, Goldblatt PJ, Hinton DE, Lipsky MM, Chacko J, Trump BF. Mouse liver cell culture. I. Hepatocyte isolation. *In Vitro* 1981; **17**: 913–925.



**Cell Death and Disease** is an open-access journal published by Nature Publishing Group. This work is licensed under a Creative Commons Attribution-NonCommercial-ShareAlike 3.0 Unported License. The images or other third party material in this article are included in the article's Creative Commons license, unless indicated otherwise in the credit line; if the material is not included under the Creative Commons license, users will need to obtain permission from the license holder to reproduce the material. To view a copy of this license, visit <http://creativecommons.org/licenses/by-nc-sa/3.0/>

Supplementary Information accompanies this paper on Cell Death and Disease website (<http://www.nature.com/cddis>)